



# Numerical Simulation of Forced Convection Heat Transfer in Pipe using Different Nanoparticles

Musfirah Mustaffa<sup>1</sup>, Abdulhafid M A Elfaghi<sup>1,\*</sup>

<sup>1</sup> Faculty of Mechanical and Manufacturing Engineering,  
Universiti Tun Hussein Onn Malaysia, Batu Pahat, 86400, MALAYSIA

\*Corresponding Author

Received 13 June 2021;  
Accepted 7 August 2021;  
Available online 30 Oct. 2021

**Abstract:** Many industrial heating and cooling systems rely heavily on heat transfer convection. Heat convection can be passively enhanced by adding well-suspended metal nanoparticles to the water. Using Computational Fluid Dynamics, this study analyses heat transfer turbulence of  $Al_2O_3$  nanofluids in a circular pipe under a constant heat flow (CFD). The convective heat-transfer coefficient, Nusselt number, and friction factor of a nanofluid are studied as a function of Reynolds number and particle volume percent. Volume fractions of 0.5, 1.0, and 2.0 percent are found in  $Al_2O_3$  nanoparticles, with range of Reynolds number of 6000 to 12000. The numerical findings indicated that nanofluids had a better convective thermal performance than the base fluid by 11.8 percent, and the heat transfer improvement rises by particle Reynolds number and volume concentration. The results showed that the current numerical results are very similar to the prior ones.

**Keywords:** Heat transfer enhancement, CFD,  $Al_2O_3$ , Ansys Fluent

## 1. Introduction

Heat transfer is a form of thermal engineering medium concerned with the use, production, conversion, and transport of thermal power between physical systems. Heat exchangers are heat transfer devices that are used to transmit or exchange thermal energy from one substance to another. They can be found in many different shapes and sizes [1-3]. Engineers and scientists have worked hard to breach the fundamental constraints of heat conductivity in ordinary fluids by diffusing millimeter or micrometer-sized particles into liquids. Nevertheless, these particles are still considered large when diffused into fluids and this may cause clogging and erosion of pipes and channels.

Researchers are interested in increasing the thermal characteristics of fluids as technology becomes more efficient. Researchers at the University of Edinburgh have presented a novel approach for improving heat conductivity by suspending nanoparticles in a base liquid. They hope to use this technique to create nanoparticles that can be used in water [4,5]. Computers will simulate heat transport in the heat exchanger for this project. Computational Fluid Dynamics (CFD) is fluid dynamics field that use solution based on mathematics to solve and evaluate fluid flow problems. It helps to prevent waste in

manufacturing cost and time related to the production of the component [6-8]. Water is commonly used as heat transfer fluid in heat exchangers, and this may result in decrease the heat transfer rate. Therefore, to increase heat transfer rate in heat exchanger, nanofluids are used as heat transfer fluid in water to minimize pumping power of heat exchanger. By using nanoparticles in nanofluids, flow friction can be reduced resulting to an efficient heat transfer [9,10]. To improve heat transport, further study is needed in this area. The goal of this study is to see how nanoparticles affected heat transmission for different Re and volume concentration.

This research aims to study a 3D flow in circular horizontal pipe using different nanofluid concentration and different types of nanoparticles. Fluent Ansys software is used to undergo the research by using different value of Reynold's numbers to see the impacts on heat transfer improvement and thermal efficiency utilizing nanofluids. After achieving the objectives, an alternative method for the manufacturing industry can be obtained. This is because CFD simulations are inexpensive, and costs are likely to decrease.

In addition, production time of the heat exchangers can be efficiently optimized as we can repeatedly run the simulation without any limitations as physical experiments and tests can be reduced. We may theoretically replicate any physical situation involving heat exchanger heat transfer as part of this research, which will allow us to regulate the physical process and isolate certain phenomena in the study of heat exchangers.

**2. Theoretical Background**

**2.1 Heat Transfer**

Sir Isaac Newton came up with the following convection of heat transfer coefficient statement [11]:

$$q = hA(T_{sur} - T_{surr}) \tag{1}$$

$q$  = rate of heat transfer (J/s)

$h$  = heat transfer coefficient (W/m<sup>2</sup>.K)

$A$  = surface area (m<sup>2</sup>)

$T_{sur}$  = Surface temperature (K)

$T_{surr}$  = Surrounding temperature (K)

**2.2 Conduction Heat Transfer**

The transient heat conduction equation may be written as [5,6]:

$$\nabla \cdot K \nabla T = c \frac{\partial T}{\partial t} \tag{2}$$

where,

$K$  = thermal conductivity (W/m.K)

$T$  = temperature (K)

$c$  = specific heat capacity of solid/volume (J/k.m<sup>3</sup>)

$t$  = time (s)

Thermodynamic conductivity is the ability to transfer heat from one place to another. The physical constant  $K$  is used in the proportionality equation. This relates the quantity of heat traversing a unit surface area per time to the spatial temperature gradient perpendicular to the surface. In 1810, Fourier can only thoroughly clarify it.

**3. Methodology**

**3.1 Physical Model and Assumption**

A basic double-pipe heat exchanger's internal pipe is encased within an outer pipe. Cold and hot fluids move in opposing directions in a counterflow system.

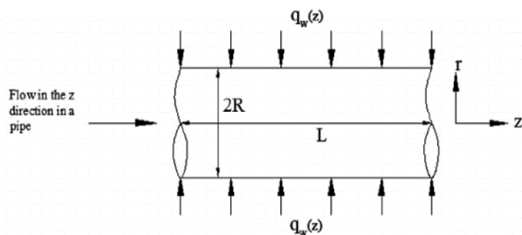


Fig. 1 - Schematic diagram of circular pipe

A computational fluid dynamic (CFD)-based numerical model is utilized to analyze properties of the nanofluid heat transfer. The 3D computational domain is utilized to account for the impact of the uniform heat flow boundary condition. The tube measures 2 meters in length and has a 5 mm inner diameter and a 6 mm outer diameter. Heat flux is constant at outer pipe wall to complete the research of heat transfer of water and Al<sub>2</sub>O<sub>3</sub> using commercial software ANSYS.

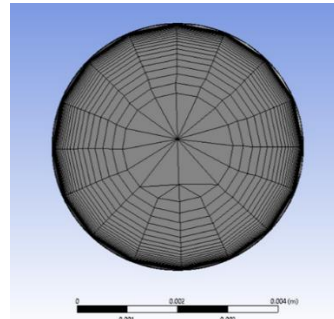


Fig. 2 - Mesh geometry of circular pipe

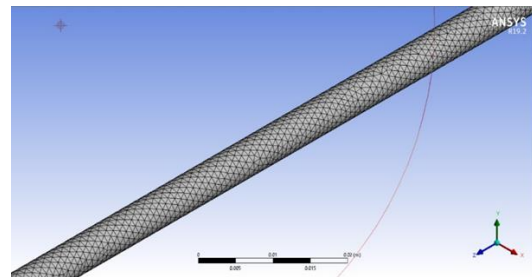


Fig. 3 - Meshing geometry of circular pipe wall

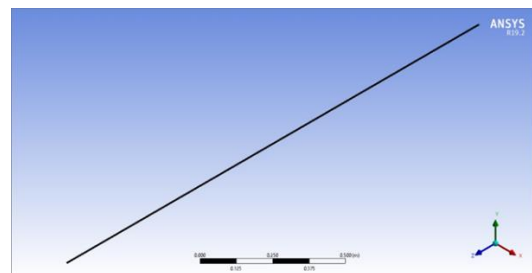


Fig. 4 - Meshing geometry of circular pipe wall

**3.2 Thermophysical Properties of Water and Al<sub>2</sub>O<sub>3</sub> Nanofluid**

Table 1 shows the water and Al<sub>2</sub>O<sub>3</sub> characteristics, and the proposed nanoparticles, Al<sub>2</sub>O<sub>3</sub>. The thermophysical characteristics formulas are shown in the section below.

**Table 1 – Thermophysical characteristics of Al<sub>2</sub>O<sub>3</sub> nanofluid**

Property	Water	TiO <sub>2</sub>
Density (kg/m <sup>3</sup> )	998.2	3970
Specific heat (J/kg.K)	4182	765
Thermal conductivity (W/m.K)	0.6	40
Viscosity (Pa.s)	0.001	-

Nanoparticle volume fraction in nanofluid,

$$\nabla \cdot K \nabla T = c \frac{\partial T}{\partial t} \tag{3}$$

Density of nanofluid,

$$\rho_{nf} = (1 - \phi)\rho_{bf} + \phi\rho_{np} \quad (4)$$

Specific heat of nanofluid,

$$c_{p,nf} = \frac{(1 - \phi)\rho_{bf}c_{p,bf} + \phi\rho_{np}c_{p,np}}{\rho_{nf}} \quad (5)$$

Thermal conductivity of nanofluid,

$$\frac{k_{nf}}{k_{bf}} = \frac{(k_{np} + 2k_{bf}) - 2\phi(k_{bf} - k_{np})}{(k_{np} + 2k_{bf}) + \phi(k_{bf} - k_{np})} \quad (6)$$

Viscosity of nanofluid,

$$\mu_{nf} = \mu_{bf} \frac{1}{(1 - \phi)^{2.5}} \quad (7)$$

Based on the equations above, volume fraction of nanoparticle  $\phi$ ,  $V_{bf}$  is base fluid volume,  $V_{np}$  as the volume of nanoparticle. Other than that,  $\rho_{np}$  is the nanoparticle's density while  $\rho_{bf}$  is the base fluid's density. The specific heat is  $C_{p,nf}$  for nanofluid while  $C_{p,bf}$  is for base fluid,  $k_{nf}$  represents the nanofluid thermal conductivity while  $k_{bf}$  is the base fluid's thermal conductivity,  $k_{np}$  is nanoparticle's thermal conductivity. Lastly,  $\mu_{nf}$  and  $\mu_{bf}$  is viscosity of nanofluid and base fluid respectively [12].

## 4. Results and Discussion

### 4.1 Nusselt number of Al<sub>2</sub>O<sub>3</sub> and TiO<sub>2</sub> nanofluids

The data comparison is based on findings reported by M.H. Kayhani et al. for the identical geometry and boundary conditions [13]. The experimental findings with various Reynolds numbers are then compared to the Nusselt number ( $Nu$ ) and heat transfer for each volume fraction ( $Re$ ). The findings of the experiment were predicated on a steady heat flow throughout the pipe. When the Reynolds number grows, the Nusselt number rises, and the coefficient of heat transfer climbs with it, according to both experimental and numerical evidence. The discrepancy between simulated findings using Al<sub>2</sub>O<sub>3</sub> nanofluid and experimental results using TiO<sub>2</sub> nanofluid is seen in this graph. Because the Nusselt number is proportional to the coefficient of heat transfer for each working fluid, its fluctuation pattern is comparable to that of the coefficient of heat transfer.

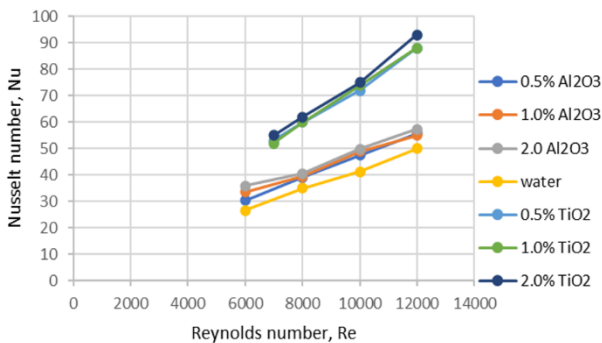


Fig. 5 - Comparison of the numerical model for Nusselt number at different Reynolds number

### 4.2 Heat transfer coefficient of Al<sub>2</sub>O<sub>3</sub> and TiO<sub>2</sub> nanofluids

A comparison of modeling and prior experimental results, as shown in Fig, suggests a comparison of the coefficient of heat transfer for both Al<sub>2</sub>O<sub>3</sub> and TiO<sub>2</sub> nanofluids increase [14].

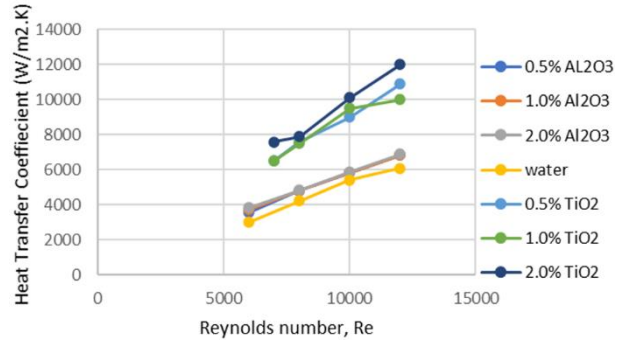


Fig. 6 - Comparison of heat transfer coefficient of Al<sub>2</sub>O<sub>3</sub> and TiO<sub>2</sub> nanofluids with water at different Reynolds number

All working fluid heat transfer coefficients have increased as the Reynolds number has increased, according to the data above, and the variation patterns are linear with rising Reynolds number, Saedodin *et al.* found a developing linear trend in heat transfer coefficient for several working fluids flowing through tubes [15].

### 4.3 Comparison of Al<sub>2</sub>O<sub>3</sub> nanofluid properties with previous study

The heat transfer parameters of Al<sub>2</sub>O<sub>3</sub> nanofluids are compared, which includes thermal properties such as heat transfer coefficient and Nusselt number, friction factor, and pressure drop. Equations provided are utilized to calculate the density, specific heat, thermal conductivity, and viscosity of Al<sub>2</sub>O<sub>3</sub> nanofluids.

Table 2 – Properties of Al<sub>2</sub>O<sub>3</sub> nanofluid at different volume concentrations

Nanofluid	Density (kg/m <sup>3</sup> )	Specific Heat (J/kg.K)	Thermal Conduct. (W/m.K)	Viscosity (Pa.s)
0.5% Al <sub>2</sub> O <sub>3</sub>	1013.06	4115.04	0.6086	0.00101
1.0% Al <sub>2</sub> O <sub>3</sub>	1027.92	4050.02	0.6174	0.00103
2.0% Al <sub>2</sub> O <sub>3</sub>	1057.64	3925.46	0.6351	0.00105

Fig 7 to 9 shows Al<sub>2</sub>O<sub>3</sub> nanofluid and water heat transfer coefficient within pipe is compared for various Reynolds number and fraction for both present simulation and the prior work. All working fluid heat transfer coefficients have grown when the Reynolds number rises, and the variation trends are linear. For current study, for 2.0% Al<sub>2</sub>O<sub>3</sub> nanofluid the coefficient of heat transfer increases by 56.28% during the increment of Reynolds number from 6000 to 12000 while 99.89% increment shown in previous study. The difference in percentage of heat transfer coefficient between the previous study with the present study is may be caused by the slight error in simulation meshing parameters, boundary conditions, initial conditions, and geometry of the circular tube.

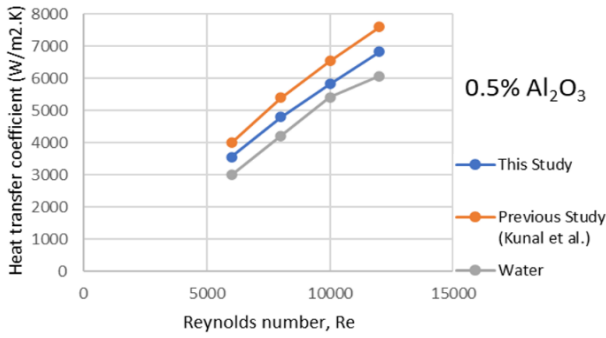


Fig. 7 - Comparison of heat transfer coefficient for 0.5% Al<sub>2</sub>O<sub>3</sub> volume fraction

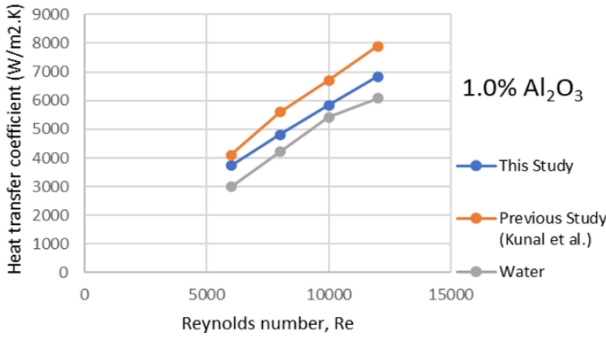


Fig. 8 - Comparison of heat transfer coefficient for 1.0% Al<sub>2</sub>O<sub>3</sub> volume fraction

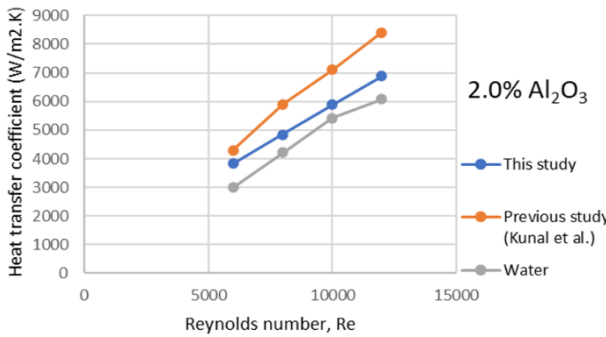


Fig. 9 - Comparison of heat transfer coefficient for 2.0% Al<sub>2</sub>O<sub>3</sub> volume fraction

The Nusselt number of various working fluids was compared to the Reynolds number in Fig. 10, 11 and 12. Coefficient of heat transfer determines the Nusselt number. This results in the Nusselt number's fluctuation trend is comparable to coefficient of heat transfer for each working fluid.

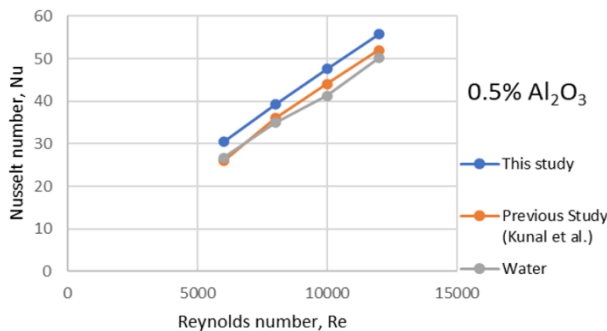


Fig. 10 - Comparison of Nusselt number for 0.5% Al<sub>2</sub>O<sub>3</sub> volume fraction

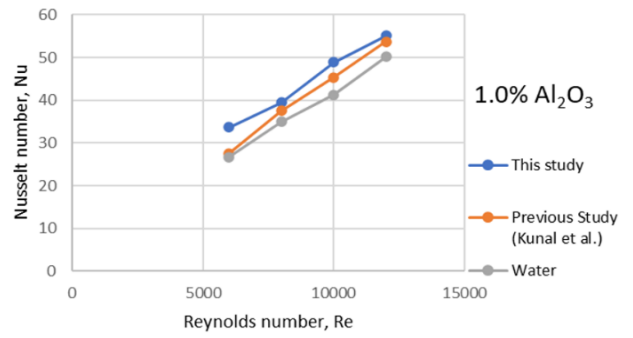


Fig. 11 - Comparison of Nusselt number for 1.0% Al<sub>2</sub>O<sub>3</sub> volume fraction

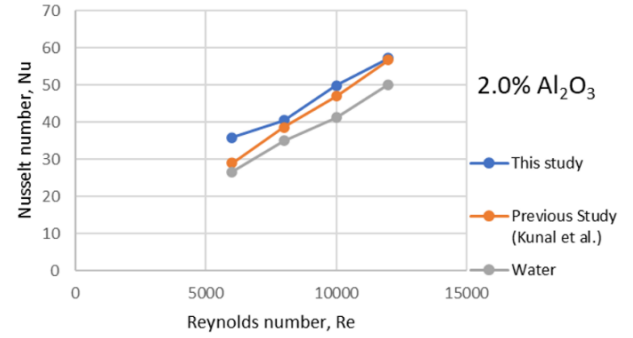


Fig. 12 - Comparison of Nusselt number for 2.0% Al<sub>2</sub>O<sub>3</sub> volume fraction

For current and prior studies of Al<sub>2</sub>O<sub>3</sub> nanofluid, the volume fraction increases and the Nusselt number rises. As the Reynolds number rises from 6000 to 12000, the Nusselt number of a 0.5% Al<sub>2</sub>O<sub>3</sub> nanofluid rises from 30.481 to 35.887. In previous work, the Nusselt number of a 0.5% Al<sub>2</sub>O<sub>3</sub> nanofluid increases from 26 to 29 when the Reynolds number rises from 6000 to 12000. The formulae below from Dittus and Boelter [16], as well as Pak and Cho [17], are used to determine the Nusselt number of Al<sub>2</sub>O<sub>3</sub> nanofluids. The Nusselt number from the simulation results may be compared to the theoretical equation expressed using these formulae.

Pak and Cho's equation for nanofluid,

$$Nu = 0.021 Re^{0.8} Pr^{0.5} \tag{8}$$

Dittus and Boelter's equation for nanofluid:

$$Nu = 0.023 Re^{0.8} Pr^{0.4} \tag{9}$$

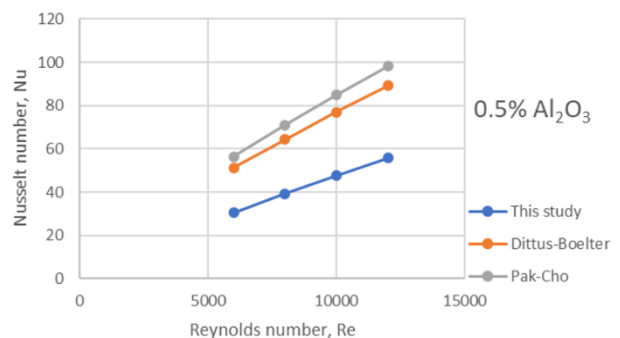
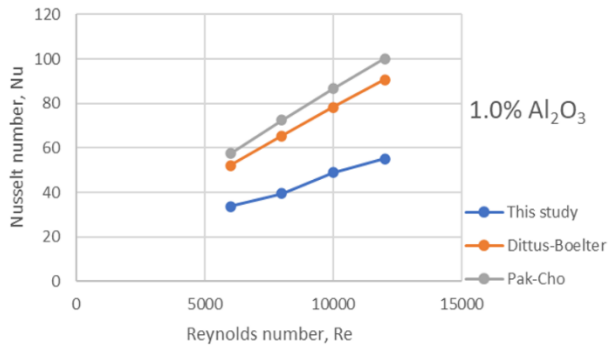
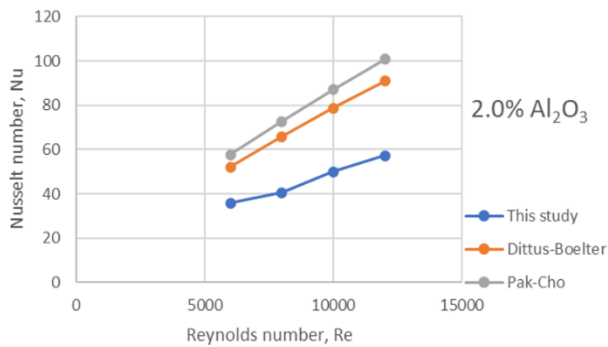


Fig. 13 - Comparison of Nusselt number between present study, Dittus and Boelter equation and Pak and Cho equation for 0.5% Al<sub>2</sub>O<sub>3</sub> volume fraction



**Fig. 14 - Comparison of Nusselt number between present study, Dittus and Boelter equation and Pak and Cho equation for 1.0% Al<sub>2</sub>O<sub>3</sub> volume fraction**



**Fig. 15 - Comparison of Nusselt number between present study, Dittus and Boelter equation and Pak and Cho equation for 2.0% Al<sub>2</sub>O<sub>3</sub> volume fraction**

To validate the computational model, the computed data from specific real correlations is compared to the assessed numerical findings. Referring to data from the graph in Fig. 13 to 15 proved that Nusselt number is affected by Reynolds number. Volume fractions increment also affects the increase of Nusselt number.

#### 4.4 Friction Factor

The effect of volume fraction and Reynolds number on the friction factor of water and Al<sub>2</sub>O<sub>3</sub> nanofluid is shown in Fig. 16. Al<sub>2</sub>O<sub>3</sub> nanofluid has greater friction factors than water, which rise as the volume fraction increases. This happens due to Al<sub>2</sub>O<sub>3</sub> nanofluids have greater viscosity than water, which rises with volume fraction.

The density of Al<sub>2</sub>O<sub>3</sub> nanofluid is greater than that of water, resulting in a lower velocity of Al<sub>2</sub>O<sub>3</sub> nanofluid. Among Al<sub>2</sub>O<sub>3</sub> and water, the 2.0% Al<sub>2</sub>O<sub>3</sub> nanofluid had the greatest friction factor. As the Reynolds number rises from 6000 to 12000, the friction factor of a 2.0% Al<sub>2</sub>O<sub>3</sub> nanofluid rises by 0.001%.

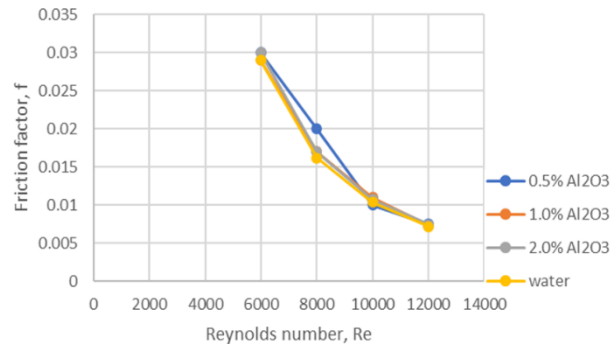


**Fig. 16 - Comparison of friction factor between present study and water**

#### 5. Conclusion

Turbulence increases as the recovery rate increases for all working fluids. The coefficient of heat transfer and Nusselt number for Al<sub>2</sub>O<sub>3</sub> nanofluid rise as the volume fraction and Reynolds number increased. Coefficient of heat transfer of 2.0% Al<sub>2</sub>O<sub>3</sub> is 11.8% than water. In the 2.0% Al<sub>2</sub>O<sub>3</sub> nanofluid, Nusselt values of 35.89 were discovered. Next, high volume fraction causes friction factor to increase. When compared to water, the 2.0% Al<sub>2</sub>O<sub>3</sub> has a 3.61% greater friction factor. In conclusion, the addition of Al<sub>2</sub>O<sub>3</sub> nanoparticles has been proved to enhance the heat transfer because of its superior thermophysical properties compared to water.

#### Acknowledgement

The author would also like to thank the Faculty of Mechanical and Manufacturing Engineering, Universiti Tun Hussein Onn Malaysia, and Flow Analysis, Simulation and Turbulence Research Group (FASTREG) for its support.

#### References

- [1] Rehman, U.U., "Heat Transfer Optimization of Shell-and-Tube Heat Exchanger through CFD Studies, Master Thesis, (2011): 25–26
- [2] Gay, J.J., and Mackley, B., "Shell-Side Heat Transfer in Baffled Cylindrical Shell and Tube Exchangers: An Electrochemical Mass Transfer Modelling Technique," *Int J Heat Mass Transfer*, 19 (1976): 995–1002
- [3] Ozden, E., and Tari, I., "Shell Side CFD Analysis of a Small Shell-and-Tube Heat Exchanger," *Energy Conversion and Management*, 51(5) (2020): 1004 – 1014
- [4] Masuda, H., et. al., "Alteration of Thermal Conductivity and Viscosity of Liquid by Dispersing Ultra-Fine Particles. Dispersion of Al<sub>2</sub>O<sub>3</sub>, SiO<sub>2</sub> and TiO<sub>2</sub> Ultra-Fine Particles," *Netsu Bussei*. 7(4) (1993): 227–233.
- [5] Wen, D., and Ding, Y., "Formulation of Nanofluids for Natural Convective Heat Transfer Applications." *International Journal of Heat and Fluid Flow*, 26(6) (2005): 855.
- [6] Khosravi, M., Mosaddeghi, F., and Oveisi, M. "Aerodynamic Drag Reduction of Heavy Vehicles using Append Devices by CFD Analysis." *J. Cent. South Univ.* 22 (2015): 4645–4652
- [7] Meyer, Josua & Vyver, H. "Validation of a CFD Model of a Three-Dimensional Tube-in-Tube Heat Exchanger." *Proceedings of the 3rd International Conference on CFD in the minerals and process industries*. Melbourne, Australia
- [8] Narasimhan, T.N., "Fourier's Heat Conduction Equation: History, Influence and Connections," *Proc. Indian Acad. Sci. Earth Planet. Sci.* 108 (1999) 117–148.

- [9] Ambekar A.S., Sivukumar R., Anantharaman N., Vivekenandan M., "CFD Simulation Study of Shell and Tube Heat Exchangers with Different Baffle Segment Configurations," *Applied Thermal Engineering*, 108 (2016): 999-1007.
- [10] Batalha Leoni G., Suaiden Klein T., de Andrade Medronho R., "Assessment with Computational Fluid Dynamics of the Effects of Baffle Clearances on the Shell Side Flow in a Shell and Tube Heat Exchanger," *Applied Thermal Engineering*, 112 (2017): 497-506.
- [11] Cheng, K.C., and Fujii, T., "Isaac Newton and Heat Transfer," *Heat Transf. Eng.* 19 (1998): 9-21.
- [12] Garud, K. and Lee, M., "Numerical Investigations on Heat Transfer Characteristics of Single Particle and Hybrid Nanofluids in Uniformly Heated Tube." *Symmetry*, 13(5) (2021): 876.
- [13] Kayhani, M.H., Soltanzadeh, H., Heyhat, M.M., Nazari, M., and Kowsary, F., "Experimental Study of Convective Heat Transfer and Pressure Drop of TiO<sub>2</sub>/water Nanofluid." *International Communications in Heat and Mass Transfer*. 39(3) (2012): 456-462
- [14] Kayhani, M.H., Nazari, M., Soltanzadeh, H., Heyhat, M.M., and Kowsary, F., "Experimental Analysis of Turbulent Convective Heat Transfer and Pressure Drop of Al<sub>2</sub>O<sub>3</sub>/water Nanofluid in Horizontal Tube." *Micro & Nano Letters*, 7(2) (2012): 223-227
- [15] Saedodin, S., Zaboli, M. and Rostamian, S., "Effect of Twisted Turbulator and Various Metal Oxide Nanofluids on the Thermal Performance of a Straight Tube: Numerical Study based on Experimental Data." *Chemical Engineering and Processing - Process Intensification*, 158 (2020): 108106.
- [16] Dittus, F.W., and Boelter, L.M.K., "Heat Transfer for Automobile Radiators of the Tubular Type," Vol. 2 of *University of California Publications in Engineering*, University of California Press, 1930.
- [17] Pak. B.C., and Cho, Y.I., "Hydrodynamic and Heat Transfer Study of Dispersed Fluids with Submicron Metallic Oxide Particles," *Experimental Heat Transfer*, 11(2) (1998): 151-170